IOP Publishing Physica Scripta
Phys. Scr. 95 (2020) 055808 (8pp) https://doi.org/10.1088/1402-4896/ab7a37

Optical properties of n-type asymmetric triple δ-doped quantum well under external fields

F Ungan[1], M K Bahar[2] and M E Mora-Ramos[3,4]

[1] Department of Optical Engineering, Faculty of Technology, Sivas Cumhuriyet University, 58140 Sivas, Turkey
[2] Department of Physics, Faculty of Science, Sivas Cumhuriyet University, 58140 Sivas, Turkey
[3] Centro de Investigación en Ciencias, Instituto de Investigación en Ciencias Básicas y Aplicadas, Universidad Autónoma del Estado de Morelos, Av. Universidad 1001, CP 62209, Cuernavaca, Morelos, México
[4] Facultad de Ciencias Básicas. Universidad de Medellín, Medellín, Colombia

E-mail: fungan@cumhuriyet.edu.tr

Received 20 November 2019, revised 7 January 2020
Accepted for publication 26 February 2020
Published 5 March 2020

Abstract

We present a theoretical investigation about the the influence of external electric, magnetic and non-resonant intense laser fields on intersubband-related second harmonics generation (SHG) and the nonlinear optical rectification (NOR) coefficients in n-type asymmetric triple δ-doped quantum wells (QWs). A particular design of asymmetric triple δ-doped QW with $L_w = 200$ Å width and, respectively, in the left side, central and right side, $N_D^L = 3 \times 10^{12}$, $N_D^C = 5 \times 10^{12}$ and $N_D^R = 7 \times 10^{12}$ cm^{-2} doping concentrations is taken into account. For QWs under the combined effect of the external electric, magnetic and laser fields, the time-dependent wave equation is modified by using Kramers-Henneberger transformation and the dipole approximation. The subband energy spectra and the electronic wave functions are obtained by solving numerically the wave equation. The originality of this work can be presented as; (i) The results explain NOR and SHG characteristics of triple QW depending on external field effects in detail. The effects of the electric, magnetic and laser field on transition energies and NOR, SHG characteristics are presented detail. (ii) In addition to, the alternativeness to each other of the external fields is discussed by probing the features of SHG and NOR under the strong and weak regimes of external fields. (iii) These nonlinear optical responses to the external fields are compared, researching the optimum cases for these optical specifications. (iv) The control of SHG through the external fields in triple δ-doped QWs reveals to be easier and more precise.

Keywords: Nonlinear optical properties, Triple quantum well, Electric, magnetic and laser fields, δ-doped confinement

(Some figures may appear in colour only in the online journal)

1. Introduction

The purpose of doping in semiconductors is to execute, in a controlled manner, the change of the free carrier density in semiconductors. This process requires the ionization of involved dopant atoms which, accordingly, become an important element of scattering of charge carriers in the crystal. Such a phenomenon causes a deterioration of electronic transport properties. Looking to overcome those disadvantages, modulation doping techniques are applied during the fabrication of semiconductor heterostructures [1, 2]. In this technique, the heterostructure is grown in such a way that the localization of ionized dopants occurs sufficiently far from the main conductive channel in the system, thus avoiding

impurity-induced electron scattering. In recent times, due to both very high electron mobility and densities achieved, as well as to the research on quantum-electronic and photonic devices, the so-called δ-doping method was worked up [3–5]. It has played an important role in fabricating selectively doped $GaAs/Ga_{1-x}Al_xAs$ heterostructures. So, if the thickness of the doped layer is very small compared to the dimensions of the material, the corresponding $1D$ doping profile can be described through Dirac delta function. In that case, the thickness of the doped zone is only a few angstrom different compared to the lattice constant. Such doped structures are named as δ-doped semiconductors, and have been the source of considerable technological developments, in parallel with advanced nano-fabrication techniques. Substantial studies are available in the literature and are still underway. The energy levels of heavy and light holes in p-type δ-doped Si quantum wells (QWs) were investigated by employing the self-consistent method in the framework of the Thomas-Fermi approximation (TFA). Despite the simplicity of the approximations applied, a very good agreement with experimental results were observed [6]. The electronic properties of related structures were discussed by examining the valence band states of p-type double δ-doped QWs in Si, within the TFA as well [7]. The carrier rates in simple and double δ-doped QWs were presented, for different doping concentrations, and the analysis of inter-layer thickness for maximum mobility was performed. Among other reports, the reader may also find some other significant studies on δ-doping. For instance, the investigation of δ-doped quantum wire tunnel junction for high concentrated solar cells [8]. Besides, the analysis of nonlinear optical features of n-type asymmetric triple δ-doped GaAs QW appears in [9]. The work in [10] presents an examination of optical absorption coefficients in n-type δ-doped GaAs QWs, and the comparison between the results obtained for electronic states and the corresponding ab-initio computations. In addition, the effect of a δ-doped source to improve the performance of $In_{0.53}Ga_{0.47}As/InP$-based SGHMOSFET is highlighted [11].

On the other hand, multiple QWs are more functional compared to single ones in everything that has to do with the enhancement of quantum efficiency; which reduces drastically due to optical absorption of electron and holes. For that reason, multiple QWs play an important role in producing high efficiency laser systems [12]. The production of perovskite-based artificial multiple QWs [13], and resonant states in double and triple QWs [14] are some of the -more relevant-latest reports, due to the fact that one of the most common application areas of usage is in Quantum Cascade Lasers [15].

The spectrum of donor impurities in triple GaAs/GaAlAs QWs under the influence of external electric and magnetic fields has been studied within a variational formalism. The analysis of the influence of different geometric encompassing regimes on binding energies was carried out varying external fields and impurity position [15]. Also, electronic and optical specifications of asymmetric multiple QWs, intended for the fabrication of Quantum Cascade Lasers, were considered [16]. In this study, the differential-cross section for electron Raman scattering process was also investigated. This quantity is useful in providing detailed information about the efficiency of lasers. Furthermore, photoluminescence spectrum in an asymmetric triple QW was analyzed as a function of external magnetic field, by considering electronic and optical transitions [17]. The computation of linear optical absorption coefficients of triple δ-doped QW under external electric and magnetic fields [18], Here, it should be pointed out that the most important common result of the above mentioned studies is that δ-doping, external fields, and multiple QW parameters can modify electronic states. Thus, many optical properties can be regulated for special purposes.

Probe of nonlinear optical properties is also a requisite, due to their areas of technological application. The functionality of SHG process is better understood when considering the need of generating new frequencies from lasers with constant wavelength [19]. If a center-symmetrical crystal is considered as a source of optical nonlinearity, it is well-known that SHG does not come about due to the lack of second-order susceptibility. In order to observe the SHG event in QWs, either suitable growth methods should be used, or the quantum system is asymmetrized through, for instance, the application of external electromagnetic fields. Reports on the subject can be exemplified as follows: the investigation of SHG coefficients of asymmetric semi-exponential QW [20], and the examination of SHG change versus electric field and well parameters in symmetric and asymmetric Gaussian QWs under the external electric field [21]. In addition, the computation of SHG coefficients for a disk-shaped quantum dot under external magnetic fields was presented considering Rashba and Dresselhaus spin-orbit interactions [22].

On the other hand, the NOR process has a remarkable role in forming of the low frequency polarization of a crystal. Also, this phenomenon constitutes a significant mechanism for generating THz level radiation [23]. NOR coefficients were analyzed for different low-dimensional systems under various external effects [24, 25]. Such studies have provided a good basis for experimental studies. In this context, the latest NOR researches can be outlined as follows: the bound state energies and wave functions of a short-range topless exponential well with inverse square root were obtained analytically [26]. Then, it was determined that the resonant energy for NOR coefficient increases with increasing well depth parameter. Besides, Ungan et. al. have elucidated the electric-, magnetic- and non-resonant laser-field dependence of NOR coefficients in Woods-Saxon QWs. It results that, while NOR increases with increasing the intensity of the electric and laser field, it decreases with increasing the magnetic field strength [27].

Researches on SHG and NOR processes without external fields or with various external fields continue without pausing. This is because nonlinear optical observables such as SHG and NOR processes comprise a basis for advanced technological applications such as optical switching [28], hologram [29], laser physics [30] and optical communications [31]. With such a motivation, the present work is devoted to perform a theoretical investigation of some nonlinear optical responses in n-type asymmetric triple δ-doped quantum well

under external fields. In particular, the coefficients of SHG and NOR are calculated. The manuscript is organized as follows: Theoretical model is demonstrated in section 2. In section 3, the discussion and results are presented. Section 4 is allocated to a brief summary and conclusions.

2. Theory

We shall study the motion of a conduction band electron bound to a n-type δ-doped triple QW in GaAs, subject to the influence of external electric, magnetic and (non-resonant) laser fields. The growth direction is oriented along the z-axis. The external electric and laser fields are applied along the growth direction. Under these conditions, the Hamiltonian that determines the electron states is:

$$H = \frac{1}{2m^{\star}}(\mathbf{P} + e\mathbf{A})^2 + V_{QW}^{(DDT)}(z, \alpha_0) + eFz, \qquad (1)$$

where, $m^{\star}$ is the electron effective mass, $\mathbf{P}$ is the momentum operator for the electron, e is electron charge, c is the speed of light in the free space. $\mathbf{A}$ vector potential in equation (1) is chosen as $\mathbf{A} = (1/2)(\mathbf{B}x\mathbf{r})$ in the symmetric gauge, and in where the magnetic field is perpendicularly applied to the growth direction. Also, the magnetic field is uniform. When $\mathbf{P}$ momentum operator and $\mathbf{A}$ vector potential are used in equation (1) by considering [$\mathbf{P}$, $\mathbf{A}$] commutation, the total interaction potential including the electric, magnetic and laser field effects is obtained. Major part of the total interaction potential is $V_{QW}^{(DDT)}(z)$, and $V_{QW}^{(DDT)}(z)$ is the potential energy function describing the conduction band bending in the n-type δ-doped triple QW, given by:

$$V_{QW}^{(DDT)}(z) = -\frac{\gamma^2}{(\gamma|z - Lw/2| + z_L)^4} - \frac{\gamma^2}{(\gamma|z| + z_C)^4} - \frac{\gamma^2}{(\gamma|z - Lw/2| + z_R)^4}. \qquad (2)$$

Here, ε_r is the dielectric constant whilst $\gamma = (e^2(2m_e^*)^{3/2})/(15\pi\epsilon_r\hbar^3)$, $z_L = (2\epsilon_r\zeta^3/(\pi e^2 N_{2d}^L))^{1/5}$, $z_C = (2\epsilon_r\zeta^3/(\pi e^2 N_{2d}^M))^{1/5}$ and $z_R = (2\epsilon_r\zeta^3/(\pi e^2 N_{2d}^R))^{1/5}$ are potential parameters. As mentioned before, N_D^L, N_D^C and N_D^R are, respectively, the right, left and center δ-doping concentrations. Analytical form of $V_{QW}^{(DDT)}(z$ potential is obtained under the TFA, within the framework of $1D$ local density functional theory [32]. This approach is quite functional to modeling the electronic properties of δ-doped structures, and is much more practical compared to computation methods such as the self-consistent one [33].

The electromagnetic laser field acting on n-type triple δ-doped QW is a monochromatic linearly polarized one. It depends on the vector potential $\mathbf{A}(\mathbf{z}, t)$ via $F' = \frac{\partial A}{\partial t}$, using the Coulomb gauge $\nabla \cdot \mathbf{A} = 0$ and $\Phi(z) = 0$. Accordingly, the potential $V_{QW}^{(DDT)}(z)$ is modified through the Kramers-Henneberger transformation [34, 35], the dipole approximation [36], the Ehlotzky approximation [37, 38], the Fourier-Floquet series [39] and other mathematical procedures [40]. As a consequence, the so-called laser-dressed n-type triple δ-doped QW potential profile is obtained from:

$$V_{QW}^{(DDT)}(z, \alpha_0) = \frac{\varpi}{2\pi}\int_0^{2\pi/\varpi} V_{QW}^{(DDT)}(z + \alpha_0 \sin\varpi t)dt, \quad (3)$$

where α_0 is considered as a parameter depicting the laser field strength, and named as laser-dressing parameter. It has the following mathematical form; $\alpha_0 = \frac{eF_0}{m^{\star}(\varpi)^2}$. In addition, F_0 and ϖ are the amplitude and angular frequency of the laser field, respectively.

The energy eigenvalues and eigenfunctions of the Hamiltonian with the potential of equation (3) are calculated by employing the diagonalization method. They become crucial information for evaluating the intersubband optical response in the structure. So, in order to compute NOR and SHG coefficients, it is considered that n-type δ-doped triple QW is simultaneously put under the combined influence of a non-resonant ILF with ϖ frequency and a light field with a much smaller frequency ω. The corresponding monochromatic optical radiation field ($E(t)$) is defined by

$$\mathbf{E}(t) = \tilde{E}e^{i\omega t} + \tilde{E}e^{-i\omega t}, \qquad (4)$$

in which polarized radiation field is exerted along the growth direction of the δ-doped triple QW. Using a description based on the statistical operator, $\hat{\rho}$, the time-evolution of its matrix elements between single electron states is written as [41]

$$\frac{\partial\hat{\rho}_{ij}}{\partial t} = \frac{1}{i\hbar}[\hat{H}_0 - \hat{M}E(t), \hat{\rho}]_{ij} - \Gamma_{ij}(\hat{\rho} - \hat{\rho}^{(0)})_{ij}. \qquad (5)$$

In this expression, $\hat{\rho}^{(0)}$ is the unperturbed -equilibrium- density matrix operator. Besides, $\hat{H}_0$ is the Hamiltonian of the system without the electromagnetic field, and $-\hat{M}E(t) = -e\hat{z}E(t)$ is the perturbation term, which includes the electric dipole moment operator, $\hat{M}$. The quantity Γ_{ij} is the relaxation rate related with damping processes.

A frequent way of writing the solution of equation (5) is by putting it forward as a perturbation series,

$$\hat{\rho}(t) = \sum_{n=0}^{\infty}\hat{\rho}^{(n)}. \qquad (6)$$

Then, equation (5) becomes

$$\frac{\partial\hat{\rho}_{ij}^{(n+1)}}{\partial t} = \frac{1}{i\hbar}([\hat{H}_0, \hat{\rho}^{(n+1)}]_{ij} - i\hbar\Gamma_{ij}\hat{\rho}_{ij}^{(n+1)}) - \frac{1}{i\hbar}[ez, \hat{\rho}^{(n)}]_{ij}E(t). \qquad (7)$$

The electronic polarization due to the $E(t)$ optical field is defined as the statistical average of the electric dipole moment [42]:

$$P(t) = \frac{Tr\{\hat{\rho}\hat{M}\}}{V}, \qquad (8)$$

with V representing the volume of the system. Taking into account the expansion (6), the polarization can be expressed as a series of terms, each of them expressing a corresponding

order contribution;

$$P(t) = (\varepsilon_0 \chi_\omega^{(1)} \tilde{E} e^{i\omega t} + \varepsilon_0 \chi_0^{(2)} \tilde{E}^2 + \varepsilon_0 \chi_{2\omega}^{(2)} \tilde{E}^{(2)} e^{2i\omega t} + \varepsilon_0 \chi_\omega^{(3)} \tilde{E}^{(2)} \tilde{E} e^{i\omega t} + \varepsilon_0 \chi_{3\omega}^{(3)} \tilde{E}^{(3)} e^{3i\omega t} + ...). \quad (9)$$

Here, ε_0 is the permittivity of free space, and $\chi_\omega^{(1)}$, $\chi_0^{(2)}$, $\chi_{2\omega}^{(2)}$, $\chi_\omega^{(3)}$ and $\chi_{3\omega}^{(3)}$ are, respectively, the linear, the optical rectification, the second harmonics generation, the third order and third harmonics generation susceptibilities. From the associated order solutions, the NOR and SHG contributions are obtained in the form [41, 43]:

$$\chi_0^{(2)} = \frac{4e^3 \rho_\nu}{\varepsilon_0 \hbar^2} \mu_{01}^2 \Delta_{01} \times \frac{\omega_{10}^2 (1 + \Gamma_2/\Gamma_1) + (\omega^2 + \Gamma_2^2)(\Gamma_2/\Gamma_1 - 1)}{[(\omega_{10} - \omega)^2 + \Gamma_2^2][(\omega_{10} + \omega)^2 + \Gamma_2^2]}, \quad (10)$$

$$\chi_{2\omega}^{(2)} = \frac{e^3 \rho_\nu}{\varepsilon_0 \hbar^2} \frac{\mu_{01} \mu_{12} \mu_{20}}{(\omega - \omega_{10} - i\Gamma_3)(2\omega - \omega_{20} - i\Gamma_3)}, \quad (11)$$

where $\Delta_{01} = |\mu_{00} - \mu_{11}|$. Being φ an eigenfunction of the wave equation, $\mu_{ij} = |<\varphi_j|z|\varphi_i>|$ $(i, j = 0, 1, 2, 3)$ represents the off-diagonal dipole moment matrix elements. $\omega_{ij} = (E_i - E_j)/\hbar$ is the intersubband transition frequency; $\Gamma_k = 1/T_k$ $(k = 1, 2, 3)$ are damping terms related to lifetime of electrons involved in transition process. The difference between the electron densities in the involved transition states is given by

$$\rho_\nu = \frac{m^* k_B T}{\pi \hbar^2 L_w} \ln \left[\frac{1 + \exp[(E_F - E_0)/(k_B T)]}{1 + \exp[(E_F - E_i)/(k_B T)]} \right], \quad (12)$$

where E_F is the Fermi energy. At low temperature (near zero T), the former expression simplifies to [44].

$$\rho_\nu = \frac{m^*}{\pi \hbar^2 L_w} (E_i - E_0), \quad (13)$$

.

3. Results and discussion

The SHG and NOR responses of triple GaAs δ-doped QWs with a total width $L_w = 200$ Å are examined versus different regimes of the external electric, magnetic and laser field strengths. The values 3, 5, 7×10^{12} cm^{-2} are chosen for left, central and right doping concentrations, respectively. The numerical values of the physical parameters involved in the calculation are: $m^* = 0.067 m_0$, being m_0 the free electron mass-, $\varepsilon_{GaAs} = 12.58$, $\varepsilon_0 = 8.854 \times 10^{-12}$ C^2/Nm^2, $\Gamma_1 = 1.0$ THz, $\Gamma_2 = 5.0$ THz, and $\Gamma_3 = 7.0$ THz. In the present analysis, there are three important parameters to change. Instead of modifying structural and compositional configurations, we analyze the features of NOR and SHG coefficients as depending on the strengths of the external field tuning probes: α_0, F and $B = |\nabla \times \mathbf{A}|$.

The only difference between figures 1(a) and (d) is the application of external magnetic field. While there is no external magnetic field in figure 1(a), it is B = 10 T in figure 1(b). As seen, the increment of the magnetic field strength deepens and narrows the QW profile as from higher energy levels. This is also affected bound states localized in lower energy levels, increasing difference between their energy levels. This case is very clear in figure 1(c). As well known, the application of a magnetic field makes the single-particle spectrum completely quantized, which in turn is confirmed in our results (See figures 1(a) and (d); figure 2(c)). Due to quantization completely of single-particle, the triple QW is similar to a quantum dot. Also, in a parabolic quantum dot, the augmentation of magnetic field leads to localize bound states in higher energy levels by decreasing width of QD profile [45, 46]. Similar behavior exhibited in QW and QD due to changing of the external magnetic field causes to similar optical specifications.

Different pictures of the confining potential profile, corresponding to the original and three particular cases of field-modified configurations appear in figure 1. In each case, the graphics also include a schematic representation of the position of the lowest three allowed energy levels, together with the corresponding probability densities. The more noticeable modifications relate with the ILF and static electric field effects. In the former, the very triple well structure practically disappears, with a transition to a single -less asymmetric- well geometry. In the latter, the asymmetry is reinforced due to the strong deformation of the barriers, due to the superimposed linear potential. Essentially, the physical effect of the applied fields reduces to the modification of the potential energy of the electron in the structure. Such a change implies, in any case, the variation of the confinement conditions for the carrier in the conduction band. This causes the shift in the energy position of the allowed states. Normally, if the depth of the original QW is large enough, the ground state energy suffers a modest displacement when the external field probe is switched on (in our cases, there is a small rise in E_0). Even so, the shape of the associated wave function might be significantly altered if the symmetry of the confining potential is varied. However, the upper levels do suffer a notable displacement which depends on the very shift of the QW bottom and the variation of the spatial confinement within it, both induced by the external field effect. Choosing one case as example, the application of a static electric field leads to the overall reduction of the spatial localization. As noticed from figure 1(c), this produces a decrease of the energy of the second excited state in the system. This kind of phenomenon is better illustrated by observing the trend of the intersubband transition energies depicted in figure 2. This figure presents the variation of the these quantities (having the ground state as the initial one) as functions of the field intensities. Increasing the ILF strength has opposite influences: the main intersubband energy transition, $E_1 - E_0$, augments whilst $E_2 - E_0$ decreases. This is a result of the narrowing of the bottom well region of the dressed potential, added to its overall widening for higher energies.

As mentioned, the effect of the static electric field, F, produces a general reduction of the transition energies, with lesser variation in the case of the main one. The increment in the intensity, B, of the applied magnetic field provides an additional reinforcement of the confinement, in such a way

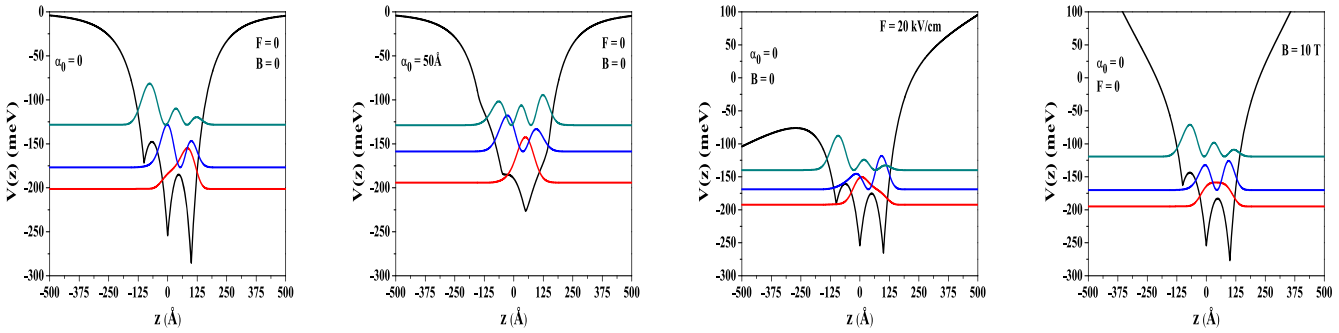

Figure 1. The plot of the potential profile and the lowest three bound states of n-type asymmetric triple δ-doped QW with $L_w = 200$ Å width and $N_D^L = 3 \times 10^{12}$, $N_D^C = 5 \times 10^{12}$ and $N_D^R = 7 \times 10^{12}$ cm^{-2} doping concentrations as a function of growth direction (a) when $\alpha_0 = 0$, $F = 0$ and $B = 0$, (b) when $\alpha_0 = 50$ Å, $F = 0$ and $B = 0$, (c) when $\alpha_0 = 0$, $F = 20$ kV cm^{-1} and $B = 0$, (d) when $\alpha_0 = 0$, $F = 0$ and $B = 10$ T.

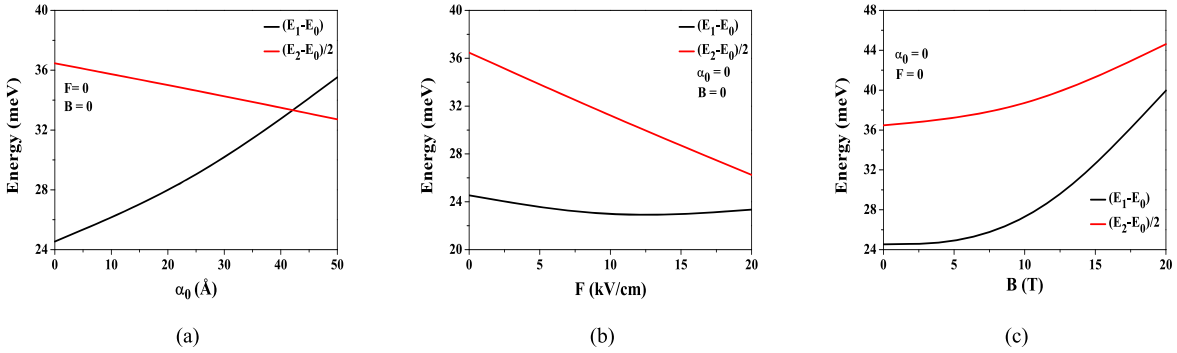

Figure 2. Intersubband transition energies $(E_1 - E_0)$ and $(E_2 - E_0)/2$ as functions of (a) α_0 for $F = 0$ and $B = 0$, (b) F for $\alpha_0 = 0$ and $B = 0$, (c) B for $\alpha_0 = 0$ and $F = 0$.

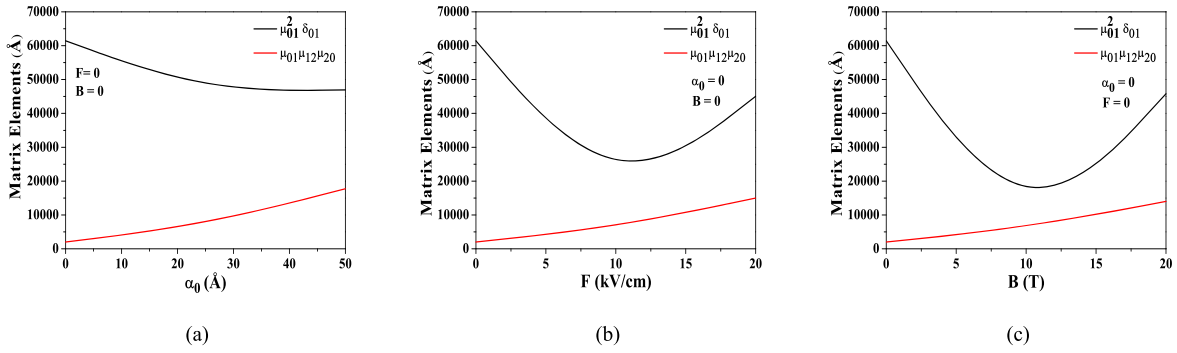

Figure 3. Matrix elements as a function of (a) α_0 for $F = 0$ and $B = 0$, (b) F for $\alpha_0 = 0$ and $B = 0$, (c) B for $\alpha_0 = 0$ and $F = 0$.

that the excited states significantly shift towards larger energy values. As a consequence, both transition energies are increasing functions of B.

Observing the figure 3, one may realize that the geometric factor responsible for the NOR peak amplitude, $\mu_{01}^2 \delta_{01}$, is a decreasing function of α_0, stabilizing its value above 35 Å. The same quantity shows an initial reduction of its value when both F an B augment, and then exhibit an increment as long as the field strengths rise. However, the amplitude factor for the SHG coefficient, $\mu_{01}\mu_{12}\mu_{20}$, always shows a growing behavior.

The information provided by the commented changes in the transition energies and amplitude factors forms the basis for the physical interpretation of the results obtained for the nonlinear optical coefficients. The outcome of the calculation for that corresponding to NOR is plotted in figure 4, as a function of the frequency of the incident light. As noticed from equation (10), the position of the resonant peak is, in this case, governed by the main intersubband transition, $E_1 - E_0$. The $E_1 - E_0$ energy gap increases nearly linearly as a result of increasing laser field strength, as seen in figure 2(a). This increment leads to blue-shift in NOR resonant frequencies, as

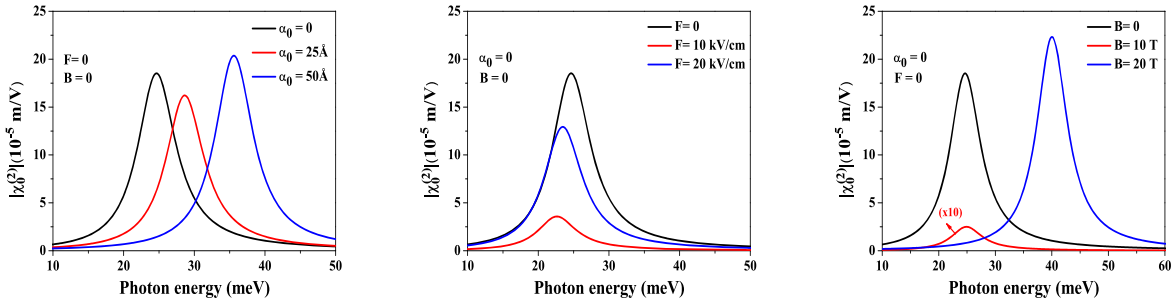

(a) (b) (c)

Figure 4. NOR coefficients as function of the incident photon energy for (a) $\alpha_0 = 0$, 25 and 50 Å when $F = 0$ and $B = 0$, (b) $F = 0$, 10 and 20 kV cm^{-1} when $\alpha_0 = 0$ and $B = 0$, (c) $B = 0$, 10 and 20 T when $\alpha_0 = 0$ and $F = 0$.

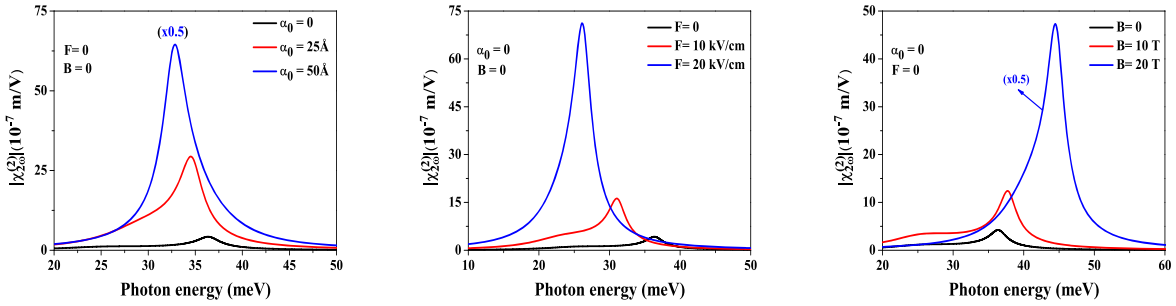

(a) (b) (c)

Figure 5. SHG coefficients as function of the incident photon energy for (a) $\alpha_0 = 0$, 25 and 50 Å when $F = 0$ and $B = 0$, (b) $F = 0$, 10 and 20 kV cm^{-1} when $\alpha_0 = 0$ and $B = 0$, (c) $B = 0$, 10 and 20 T when $\alpha_0 = 0$ and $F = 0$.

seen in figure 4(a). The $\mu_{01}^2\delta_{01}$ matrix elements decrease monotonically and then increase weakly (See figure 3(a)), which in turn leads to a similar oscillation in NOR amplitudes (See figure 4(a)). More clearly, the NOR amplitude, in this case, has an initial fall that can be associated to the decrease of the geometric factor observed in figure 3(a) when $\alpha_0 < 30$ Å. The ulterior growth in the NOR, for larger values of the ILF parameter, has to do with the stabilization of the geometric factor and the increment of the relative volume density of electrons, according to equation (13), due to the blue-shift commented.

The relatively slight shift of the NOR signal to lower frequencies and its subsequent return towards larger photon energies depicted in figure 4(b) has its explanation in the smooth variation of $E_1 - E_0$ shown in figure 2(b). As the increase smoothly of the external electric field strength decreases $E_1 - E_0$ energy gap (See figure 2(b)), red-shift weakly in NOR resonant frequencies is observed (See figure 4(b)). The fact that $\mu_{01}^2\delta_{01}$ matrix elements decrease and then increase because of increasing F (See figure 2(b)) reflects to corresponding amplitudes exactly (See figure 4(b)). Finally, in the figure 4(c), we show the behavior of the calculated NOR coefficient when there is an external magnetic field acting upon the system. The initially slow increment in the main transition energy noticed in figure 2(c) is responsible for the slight shift of the resonant peak position towards higher energies for $B = 10$ T. But, for stronger fields, a significant blue-shift is revealed. This is consistent with the strong growth of E_{10} reported in such a field intensity region. Moreover, the very large reduction in the NOR amplitude associated to the great fall experienced by $\mu_{01}^2\delta_{01}$ when $B < 10$ T (see figure 3(b)) is reversed for bigger magnetic fields. This is due to the combination of the increments in the geometric factor and the relative electron volume density.

In figure 5(a) contains the SHG coefficient as a function of the photon energy when $F = 0$ and $B = 0$. In this case, the values $\alpha_0 = 0$, 25 and 50 Å are introduced as parameters. As a three-level phenomenon, both $E_1 - E_0$ and $E_2 - E_0$ transition energies are involved. As noticed from figure 2(a), the second transition energy goes down linearly with α_0 due to the transition from the triple QW to a wider single well profile when augmenting α_0 (See figure 1(b)). This, in turn, leads to a redshift in SHG main resonant peak, as can be seen in figure 5(a). However, the increment of the product of intersubband dipole matrix elements, noticed in figure 3(a) as a function of α_0, induces the steady increase of the SHG amplitude seen in figure 5(a).

When $\alpha_0 = 0$ and $B = 0$, the SHG coefficient for $F = 0$, 10 and 20 kV cm^{-1} is shown in figure 5(b), as a function of incident photon energy. A linear decrease in the $E_2 - E_0$ transition energy, as a result of that the increment of the external electric field strength (see figure 1(c)), leads to a stable red-shift in resonant frequencies. This can be noticed from figure 2(b). Similarly, the quasi-linear behavior with F exhibited by the product of intersubband matrix elements in figure 3(b) is responsible for the particular degree of enhancement in SHG amplitudes depicted in figure 5(b). On the other hand, in figure 5(c) (case with $\alpha_0 = 0$ and $F = 0$),

the SHG coefficient for $B = 0{,}10$ and 20 T are demonstrated as a function of the incident photon energy. The increasing behavior of the intersubband transition energies seen in figure 2(c) –related with magnetic-field-induced stronger confinement (compare figures 1(a) and (d))–causes the blue-shift in SHG resonant frequencies. Furthermore, augmenting B enhances SHG resonant peak amplitude due to the growing linear dependence of $\mu_{01}\mu_{12}\mu_{20}$ with the magnetic field strength, as appreciated from figure 3(c).

4. Conclusions

In this work, the effects of of the external electric, magnetic and laser field on SHG and NOR responses in n-type asymmetric triple δ-doped QW with $L_w = 200$ Å width and $N_D^L = 3 \times 10^{12}$, $N_D^C = 5 \times 10^{12}$ and $N_D^R = 7 \times 10^{12}$ cm^{-2} doping concentrations are probed for the first time.

The most remarkable outcomes of the study can be outlined as follows:

- (i) While the strengthening of the external magnetic field and laser field enhance the nonlinear optical responses of asymmetric triple δ-QW, the external electric field acts as opposite. It is worth to highlight that the latter is, precisely, the external factor that greatly breaks the symmetry of the system. However, the magnetic field reinforces the carrier confinement.
- (ii) Due to the arising geometry of the confining potential, the augmentation of the laser field intensity increases the main intersubband transition energy. On the contrary, such a rise provokes the reduction of $E_2 - E_0$ one. However, the enhancement of F and B creates a similar impact for those two energy transitions. That is, both behave as decreasing with increasing F and behave as increasing with growing B.
- (iii) While the product of electric dipole moment matrix elements involved in the NOR coefficient exhibit an undulation dependently on the enhancement of external field strength, that contained in the SHG coefficient reacts linearly (or quasi-linearly) in any case. Those features reflect in the behavior of the associated response amplitudes.
- (iv) It turns out that the external parameters α_0 and B are alternative to each other in order to tuning NOR resonant frequency. At the same time, α_0 and F are alternative to each other in tuning of SHG one.
- (v) Regarding the amplitude of the calculated coefficients, it becomes apparent that alternative parameter analysis for NOR amplitudes is not recommendable, because of the lack of single monotony of the product of matrix elements as functions of the external fields. But, it is clear that the electric, magnetic and laser fields are alternative to each other in raising the SHG amplitudes.
- vi) Given the functionality of the external fields, it is concluded that n-type asymmetric triple δ-doped QW structure is preferable and more stable for generating a frequency doubling in triple asymmetric δ-QW rather than for optical rectification. In fact, the SHG profile holds a case with both higher peak and is stable under the enhancing strengths of the external fields. But, as can be seen clearly in NOR profiles, the enhancement of the optical rectification response of triple δ-QW structure is not uniform for the all the external fields. Accordingly, it can be said that triple QW structure in consideration of frequency doubling is more optimum for stronger regimes of the external fields.

In accordance, we think that the outcome of the present work ensures significant data for device design and applications involving SHG and NOR characteristics of n-type asymmetric triple δ-doped QW, with advantages for technological applications.

Acknowledgments

MEMR is grateful to Universidad de Medellín for hospitality and support during sabbatical stay. He also acknowledges Mexican CONACYT for support through Grant CB A1-S-8218.

ORCID iDs

F Ungan https://orcid.org/0000-0003-3533-4150
M K Bahar https://orcid.org/0000-0003-4265-1402
M E Mora-Ramos https://orcid.org/0000-0002-6232-9958

References

[1] Dingle R, Störmer H L, Gossard A C and Wiegman W W 1978 *Appl. Phys. Lett.* **33** 665
[2] Störmer H L, Dingle R, Gossard A C, Wiegman W W and Sturge M D 1979 *J. Vac Sci. Technol.* **16** 1517
[3] Ke M L, Rimmer J S, Hamilton B, Evans J H, Missous M, Singer K E and Zalm P 1992 *Phys. Rev.* B **45** 14114
[4] Nakazato K, Blaikie R J and Ahmed H 1994 *J. Appl. Phys.* **75** 5123
[5] Osvald J 2004 *Physica* E **23** 147
[6] Gaggero-Sager L M and Mora-Ramos M E 2000 *Solid-State Electron.* **44** 1
[7] Rodríguez-Vargas I and Gaggero-Sager L M 2005 *Phys. Status Solidi* **2** 3634
[8] Bahrami A *et al* 2019 *Chin. Phys.* B **28** 046102
[9] Ungan F, Pal S, Bahar M K and Mora-Ramos M E 2019 *Superlattices Microstruct.* **130** 76
[10] Noverola-Gamas H, Gaggero-Sager L M and Oubram O 2019 *Int. J. Mod. Phys.* B **33** 1950215
[11] Mohanty S S, Mishra S, Mohanty S and Mishra G P 2019 *Devices for Integrated Circuit (DevIC)* (Piscataway, NJ: IEEE) pp. 53 978-1-5386-6723-1
[12] Dai Q *et al* 2009 *Appl. Phys. Lett.* **94** 111109
[13] Lee K J *et al* 2019 *Nano Lett.* **19** 3535
[14] Tanimu A and Muljarov E A 2018 *Journal of Physics Communications* **2** 115008
[15] Pacheco M, Barticevic Z and Latge A 2001 *Physica B* **302** 77
[16] Betancourt-Riera R, Rosas R, Marin-Enriquez I, Riera R and Marin J L 2005 *J. Phys. Condens. Matter* **17** 4451

[17] Fukuta S, Goto H, Sawaki N, Suzuki T, Ito H and Hara K 1993 *Semicond. Sci. Technol.* **8** 1881
[18] Restrepo R L, Castano-Vanegas L F, Martínez-Orozco J C, Morales A L and Duque C A 2019 *Appl. Phys.* A **125** 31
[19] Koechner W 1965 *Solid-State Laser Engineering* (Berlin: Springer) pp. 507
[20] Mou S, Guo K, Liu G and Xiao B 2014 *Phys.* B **434** 84
[21] Yuan J H, Chen N, Mo H, Zhang Y and Zhang Z H 2015 *Superlatt. Micro.* **88** 389
[22] Nautiyal V V and Silotia P 2018 *Phys. Lett.* A **382** 2061
[23] Tonouchi M 2007 *Nature Photon.* **31** 97
[24] Razzari L *et al* 2009 *Phys. Rev.* B **79** 193204
[25] Danielson J R, Lee Y S, Prineas J P, Steiner J T, Kira M and Koch S W 2007 *Phys. Rev. Lett.* **99** 237401
[26] Yu Q, Guo K and Hu M 2019 *Sci. Rep.* **9** 2278
[27] Ungan F, Mora-Ramos M E, Yesilgul U, Sari H and Skmen I 2019 *Phys.* E **111** 167
[28] Villeneuve A, Yang C C, Wigley P G J and Stegeman G I 1992 *Appl. Phys. Lett.* **61** 147
[29] Eaton D F 1991 *Scien.* **253** 281
[30] Laud B B 1992 *Lasers and Nonlinear Optics* (New York: Wiley)
[31] Marciniak M and Kowalewski M 2000 *J. Telecommun. Infor. Tech.* **1-2** 3 https://www.itl.waw.pl/czasopisma/JTIT/2000/1-2/3.pdf
[32] Ioriatti L 1990 *Phys. Rev.* B **41** 8340
[33] Gaggero-Sager L M and Perez-Alvarez R 1995 *J. Appl. Phys.* **78** 4566
[34] Kramers H A 1956 *Collected Scientific Paper* (Amsterdam: North-Holland)
[35] Henneberger W C 1968 *Phys. Rev. Lett.* **21** 838
[36] Bransden B H and Joachain C J 2003 *Physics of Atoms and Molecules* (Harlow: Prentice Hall)
[37] Ehlotzky F 1985 *Can. J. Phys.* **63** 907
[38] Ehlotzky F 1988 *Phys. Lett.* A **126** 524
[39] Gavrila M and Kaminski J Z 1984 *Phys. Rev. Lett.* **52** 613
[40] Bahar M K 2015 *Phys. Plasmas* **22** 092709
[41] Yu Y B and Wang H J 2011 *Superlatt. Microstr.* **50** 252
[42] Rezaei G, Vaseghi B, Taghizadeh F, Vahdani M R K and Karimi M J 2010 *Superlatt. Microstr.* **48** 450
[43] Boyd R W 2007 *Nonlinear Optics* 3rd edn (New York: Rochester)
[44] Rodriguez-Magdaleno K A, Martinez-Orozco J C, Rodriguez-Vargas I, Mora-Ramos M E and Duque C A 2014 *J. Luminescence* **147** 77
[45] Soylu A 2012 *Ann. Phys.* **327** 3048
[46] El-Said M 1995 *J. Phys. I France* **5** 1027
[47] Razeghi M 2010 *Technology of Quantum Devices* (Evanston-USA: Springer) pp. 271–321